

Erik Larsen and Ronald M. Aarts,
Philips Research, Eindhoven, The Netherlands

Presented at
the 108th Convention
2000 February 19-22
Paris, France



AES

This preprint has been reproduced from the author's advance manuscript, without editing, corrections or consideration by the Review Board. The AES takes no responsibility for the contents.

Additional preprints may be obtained by sending request and remittance to the Audio Engineering Society, 60 East 42nd St., New York, New York 10165-2520, USA.

All rights reserved. Reproduction of this preprint, or any portion thereof, is not permitted without direct permission from the Journal of the Audio Engineering Society.

AN AUDIO ENGINEERING SOCIETY PREPRINT

PERCEIVING LOW PITCH THROUGH SMALL LOUDSPEAKERS

Erik Larsen and Ronald M. Aarts

Philips Research Laboratories

Eindhoven, The Netherlands

e-mail: erik.larsen@philips.com, ronald.m.aarts@philips.com

Abstract

Since the invention of the electrodynamic loudspeaker, there has been a need for greater acoustical output, especially at low frequencies. For modern-day applications it is desirable to reduce the volume of the loudspeaker (and cabinet). These two demands are physically contradictory. It is the aim of this paper to offer options to evoke the illusion of a higher bass response, while the power radiated by the loudspeaker at those low frequencies remains the same or is even lower. This is feasible by exploiting certain psychoacoustic phenomena. The required non-linear signal processing is studied for a number of specific implementations in continuous and discrete time.

1 Introduction

In many sound reproduction applications, small loudspeakers are unavoidable, due to size and/or cost requirements. One of the most well-known characteristics of small loudspeakers is a poor low-frequency response. In practice this means that a significant portion of the audio signal may not be reproduced sufficiently by the loudspeaker. As the bass frequencies often play an important role in music, a reproduction system which is not able to reproduce these bass components will probably not be rated favorably by many listeners. Achieving a higher radiated sound pressure level by 'boosting' low frequencies is a limited solution in the sense that distortion or even damage to the loudspeaker may occur.

The rest of this paper is organized as follows: in Sec. 2 we illustrate the limitations physics impose on a small loudspeaker, in terms of its parameters. Especially in situations where cost is an issue it would be attractive if the perceived bass response of a small loudspeaker could be enhanced by some simple signal processing, without altering the loudspeaker itself. Thus, it is the goal of this paper to offer options to achieve just this.

As we get closer to or above the cut-off frequency of a loudspeaker its efficiency increases drastically and distortion is less likely to occur. Considering this fact, it would be an enormous advantage if we could enhance the perceived bass using only higher frequencies. In that case, the loudspeaker would seem to radiate a substantial

amount of energy in a region in which it actually hardly does. Now we know, from psychoacoustic theory, that a pitch sensation can exist at a frequency at which no energy is radiated by the sound source. Sec. 3 shortly reviews some conceptual possibilities to create such a low pitch perception using only higher frequencies.

In Fig. 1, we propose a signal processing algorithm consisting of a few basic operations which are required to achieve this psychoacoustic bass enhancement. A block scheme with two branches is shown in the figure; in the top signal path two bandpass filters and a non-linear device (NLD) are shown. Filter BP1 selects those frequency components which are too low to be reproduced by the loudspeaker. These bass frequencies form the input for the NLD, which creates an appropriate spectrum of higher frequencies, which may be subsequently shaped by filter BP2. In the lower signal branch, the input signal is optionally highpass filtered if distortion is a problem. Both signals are then added and fed to the loudspeaker. Depending on the design of the various filters and the specific implementation of the NLD, the radiated acoustic signal has an enhanced bass (this concept was already introduced in [1] as applied to ‘Ultra Bass’). The challenge in designing such a circuit is to control pitch, timbre and loudness of the enhanced part in some predefined way; one option is to try to re-create the original audio signal as perceived through ‘perfect’ loudspeakers. In Sec. 4, we discuss several aspects of the circuit of Fig. 1 and we give some specific examples for the NLD. We focus on time instead of frequency domain implementations. In the latter case, familiar problems such as connection of consecutive blocks after the IFFT, spectral leakage for frequencies which are not harmonic to the FFT window and non-stationarity of the input signal during the FFT window introduce significant problems.

Finally, in the appendix, we present analytical expressions for the two NLDs presented in Sec. 4, in continuous and discrete time. Using these expressions we can study the behaviour of the NLDs, for example in regard to intermodulation distortion.

2 Loudspeaker efficiency

In this section we make plausible that, for a small loudspeaker, achieving a low cut-off frequency while maintaining a reasonable efficiency is not possible with a traditional loudspeaker-cabinet construction. Reproducing frequencies below the cut-off frequency is very inefficient and should be avoided as much as possible. This provides enough motivation to investigate the possibility of creating ultra low pitch perceptions using frequencies above (or at least closer to) the cut-off frequency of the loudspeaker.

In order to show this we explore the relation between various loudspeaker parameters and radiation efficiency. For a more elaborate treatment on the radiation characteristics of various types of loudspeakers the reader is referred to Olson [2].

We first define the efficiency η at frequency ω as

$$\eta(\omega) = \frac{P_a(\omega)}{P_e(\omega)}, \quad (1)$$

where P_a is the time averaged acoustically radiated power and P_e is the time averaged electrical power supplied by the generator. We then write

$$P_a(\omega) = \frac{1}{2} \hat{V}^2 \Re\{Z_{rad}(\omega)\}, \quad (2)$$

where \hat{V} is the voice coil velocity amplitude and Z_{rad} the mechanical radiation impedance ($\Re\{\bullet\}$ denotes the real part of \bullet), and P_e is given by

$$P_e(\omega) = \frac{1}{2} \hat{I}^2 \Re\{Z_{in}(\omega)\}, \quad (3)$$

where \hat{I} is the current amplitude delivered by the generator and Z_{in} the total impedance load as seen by the generator.

Using the lumped element analogon [2, 3], we find the mobility analogous circuit of an electrodynamic loudspeaker in a closed box as shown in Fig. 2. Here, we have used the following elements:

E	generator	
R_E	resistance of voice coil	$[\Omega]$
L_E	self-inductance of voice coil	$[H]$
I	current delivered by generator	$[A]$
U	voltage across voice coil	$[V]$
V	velocity of voice coil	$[m/s]$
F	force on voice coil	$[N]$
m_1	mass of voice coil and cone	$[kg]$
k_t	total spring constant (suspension, cabinet)	$[N/m]$
R_m	mechanical damping of transducer	$[Ns/m]$
Z_{rad}	radiation impedance	$[Ns/m]$

We can now write for the impedance Z_{in} as seen by the generator

$$Z_{in}(\omega) = R_E + j\omega L_E + \frac{(Bl)^2}{R_m + R_{rad}(\omega) + j(\omega m_t(\omega) - \frac{k_t}{\omega})}, \quad (4)$$

where B is the magnetic inductance ($[T]$) in the air gap and l is the length of the voice coil wire ($[m]$). R_{rad} is the real part of the complex radiation impedance $Z_{rad} = R_{rad} + jX_{rad}$, where X_{rad} has been added to m_1 to form m_t , the total moving mass. Strictly speaking m_t is frequency dependent due to the contribution

of X_{rad} , but this contribution is small¹ and thus we will consider m_t to be frequency independent in the following. Combining Eqns. 3 and 4, we get

$$P_e(\omega) = \frac{1}{2} \hat{I}^2 \left\{ R_E + \frac{(Bl)^2 (R_m + R_{rad}(\omega))}{(R_m + R_{rad}(\omega))^2 + (\omega m_t - \frac{k_t}{\omega})^2} \right\}. \quad (5)$$

Next, we shall express the voice coil velocity amplitude V in I , the current delivered by the generator. We substitute the result in Eqn. 2, and then compute the efficiency η by Eqn. 1. According to $F = BIl$, the current through the voice coil determines the force F on it. The relation between F and V is determined by the mechanical impedance

$$\begin{aligned} V(\omega) &= \frac{F(\omega)}{(R_m + R_{rad}(\omega) + j(\omega m_t - \frac{k_t}{\omega}))} \\ &= \frac{BlI(\omega)}{(R_m + R_{rad}(\omega) + j(\omega m_t - \frac{k_t}{\omega}))}. \end{aligned} \quad (6)$$

Combining Eqns. 2 and 6, we find

$$P_a = \frac{1}{2} \hat{I}^2 \frac{(Bl)^2 R_{rad}(\omega)}{(R_m + R_{rad}(\omega))^2 + (\omega m_t - \frac{k_t}{\omega})^2}. \quad (7)$$

Now we can readily compute the efficiency by Eqn. 1 to be

$$\eta(\omega) = \frac{(Bl)^2 R_{rad}(\omega)}{R_E (\omega_0 m_t)^2 \left\{ \left[\frac{R_m + R_{rad}(\omega)}{\omega_0 m_t} \right]^2 + \frac{R_m + R_{rad}(\omega)}{R_E} \left[\frac{Bl}{\omega_0 m_t} \right]^2 + \left[\frac{\omega}{\omega_0} - \frac{\omega_0}{\omega} \right]^2 \right\}}, \quad (8)$$

where ω_0 is the resonance frequency of the mass-spring system, given as

$$\omega_0 = \sqrt{\frac{k_t}{m_t}}. \quad (9)$$

To study the behaviour of η for various frequencies, we first notice that according to [4, p. 9],

$$R_{rad}(\omega) = \begin{cases} \frac{\rho_0 \omega^2 S^2}{2\pi c_0} & \text{for } \omega \ll \frac{\sqrt{2}c_0}{a}, \\ \rho_0 c_0 S & \text{for } \omega \gg \frac{\sqrt{2}c_0}{a}, \end{cases} \quad (10)$$

where we denote sound velocity by c_0 , air density by ρ_0 , cone radius by a and cone area by S . The frequency at which the behaviour of R_{rad} changes is the transition

¹According to [4, p. 9], for a rigid circular piston in an infinite baffle the mechanical impedance (for frequencies much lower than the transition frequency of the piston, which equals $c_0/\pi a\sqrt{2} \approx 1.5$ kHz using the values given below) $X_{rad} = \omega m_{air} = \frac{8\rho_0 \omega S^2}{3\pi^2 a}$, with S for cone area, a for cone radius and ρ_0 for air density. We use e.g. $\rho_0 = 1.3$ kg m⁻³, $S = \pi(0.05)^2$ m² and $a = 0.05$ m, then we find for $m_{air} \approx 1$ g. Thus, from now on, we will consider m_t to be frequency independent.

frequency ω_t (above which the radiation becomes increasingly directional). We can immediately deduce from Eqns. 8 and 10 that in the normal operating range of the loudspeaker the efficiency is constant and equals

$$\eta(\omega) \approx \frac{(Bl)^2 \rho_0 S^2}{R_E 2\pi c_0 m_t^2}, \quad \omega_0 \ll \omega \ll \omega_t. \quad (11)$$

This clearly presents a problem: a high efficiency requires a large cone area and at the same time a small mass. The precise behaviour of η around ω_0 depends on the loudspeaker parameters, but it is not within the scope of this paper to investigate this now. If we focus on what happens for $\omega \ll \omega_0$, we notice that the last term between the curly braces in the denominator of Eqn. 8 is dominant and equal to $(\omega_0/\omega)^2$, and in combination with the ω^2 behaviour of R_{rad} , we thus have

$$\eta(\omega) \sim \omega^4, \quad \omega \ll \omega_0. \quad (12)$$

It is clear that the efficiency decreases rapidly below the resonance frequency of the loudspeaker. Referring to the definition of this cut-off frequency (Eqn. 9), we see that in order to achieve a low cut-off frequency we must have a low k_t and a high m_t . Since the contribution of the cabinet, k_c , to k_t is given by [3, p. 129]

$$k_c = \frac{\rho_0 c_0^2 S^2}{V_0}, \quad (13)$$

with V_0 the cabinet volume, it is obvious that for small loudspeaker enclosures, k_t will be relatively high. Furthermore, small loudspeakers obviously have a small mass; the combination of k_t and m_t for a small loudspeaker is precisely opposite to what one needs to obtain a low cut-off frequency. Increasing m_t is not really an option, because as Eqn. 11 shows, this will lead to a much lower efficiency.

3 Psychoacoustics

There are several options to increase the perception of low frequencies based on psychoacoustic events. In this section we discuss three such options.

3.1 Heterodyning

In previous studies [5–8] a frequency doubler was introduced, whereby signals in the low frequency band also appeared one octave higher. We call this ‘heterodyning’, and can be considered as one of the options. The mentioned heterodyning method, shown in Fig. 3-a has simplicity as an advantage. By means of a simple non-linear element, e.g. a diode, frequencies around f_0 , the frequency region where the loudspeaker does not radiate sufficient power, are shifted to $2f_0$. A drawback is that the pitch has been changed. Furthermore, impulsive sounds with a high low frequency content are seriously distorted. Nevertheless, experiments have shown that heterodyning can be an improvement.

3.2 Virtual pitch

Pitch is a subjective, psychophysical quantity. According to the American Standards Association pitch is “that attribute of an auditory sensation in terms of which sounds may be ordered on a scale extending from low to high”. For a pure tone, where the fundamental frequency corresponds to the frequency of the tone, the pitch is unambiguous and — if we neglect the influence of sound level on pitch— one can identify pitch with the frequency of the pure tone. For a complex tone, consisting of more than one frequency, the situation is more complicated. Pitch should then be measured by psychophysical experiments. A pitch that is produced by a set of frequency components, see Fig. 3-b, rather than by a single sinusoid, is called a *residue*. In Fig. 3-b the fundamental frequency is missing, yet will still be perceived as a residue pitch, which in this case is also called *virtual pitch*. The psychoacoustic phenomenon responsible for this effect is the ‘missing fundamental’ effect. Famous are the experiments of Seebeck in 1843, and the controversy of him with Ohm; see Plomp for a historical review [12]. There is a vast amount of literature on this topic, see e.g. [13–19] to name just a few. Only sparse data is known for (very) low frequencies, say < 100 Hz. Ritsma’s papers [16, 17] discuss the existence region of the tonal residue for $f > 200$ Hz.

3.3 Difference tone

Firstly, we will have a digression on organ pipes. The idea is, if there is not enough space (in a church) for a pipe long enough to produce very low notes, one can combine two higher notes to get a similar perceptual effect. This principle was — according to Helmholtz [9] — discovered in 1745 by Sorge, a German organist, however, this is often known as Tartini’s tones. Since the end of the sixteenth century, many organs include a stop (the “ $5\frac{1}{3}$ -foot fifth”) composed of pipes sounding a fifth higher than the pitch of the actual note as played from the musical score. The purpose is to stimulate or reinforce the bass one octave below the pitch of the actual note (that is, to reinforce the 16-foot sound of the organ). Of older use, (according to Roederer [10], but if Helmholtz is right, it can not be older) is the use of the $10\frac{2}{3}$ -foot fifth in the pedals, which in combination with 16-foot stops, evokes the 32-foot bass. Roederer [10] attributes this as residue pitch (Fig. 3-b), however, this is probably wrong, since the effect of residue pitch decreases very fast for low frequencies. Consequently, it is probably due to difference tones (Fig. 3-c). This is illustrated, as an example, in Table 1, showing which frequencies are obtained for the mentioned pipes. The acoustical bass concept for organs has also been considered by Terhardt and Seewann [11].

Table 1: Example of the acoustical bass of an organ. The length of the two organ pipes are L_1 and L_2 in feet (m) (without end correction term) and their corresponding individual frequencies, f_1 and f_2 . The perceived pitch is Δf , which would require a pipe of length $L_{\Delta f}$.

$L_{\Delta f}$	Δf	L_1	f_1	L_2	f_2
32' (9.75 m)	17.6 Hz	16' (4.9 m)	35.2 Hz	$10\frac{2}{3}$ ' (3.3 m)	52.7 Hz

3.4 Considerations on loudness effects

It is well-known that loudness perception depends very strongly on the frequency (range) of the stimulus that is presented to the ear(s). Fig. 4 shows the equal-loudness contours for pure tones. We clearly see that the contours lie closer together as the frequency approaches very low values; this implies that small changes in sound level lead to large changes in loudness level. We also see that for very low frequencies the hearing threshold increases rapidly.

Considering the processing proposed in Fig. 1, without at this moment requiring knowledge about the non-linear device which creates the higher frequencies, we observe that we are transposing a low frequency band ($f_1 - f_2$) to a higher region ($f_2 - f_3$). We can expect that the frequencies in the higher band will sound louder than in the original band, and also that the sensitivity for variations in loudness is greater. But there are many uncertainties if we want to quantify these effects. For instance, Fig. 4 pertains to pure tones, while in our case we will have tone complexes. Moreover, tone duration and envelope may influence loudness. Based on the well-known equal-loudness contours shown in Fig. 4, Ben-Tzur *et al.* [20] have proposed an *equal loudness level function*.

4 Generating harmonics

4.1 Processing scheme

In this section we discuss the various blocks in the general processing scheme of Fig. 1. Obviously, a good choice for the NLD is important, but also the design of the various filters is of critical importance for a good result. The complete system was implemented in C-code on a workstation, using a digital signal of a CD player.

4.1.1 First bandpass filter (BP1)

This filter selects frequencies which lie below the cut-off frequency of the loudspeaker. A typical implementation for this filter could be a bandpass filter with cut-off frequencies of 20 and 80 Hz (but should be tuned for each loudspeaker). The passband should not be too broad, otherwise intermodulation distortion can become audible in the non-linear device. If a larger bandwidth must be processed an

option could be to split this filter in several narrower filters, which then pass their output to a corresponding number of NLDs.

4.1.2 Non-linear device (NLD)

In this element the input frequencies are transposed to a higher frequency region. Keeping the original pitch can be achieved if this non-linear device is a harmonics generator. Due to the missing fundamental and/or difference tone effect described in Sec. 3, the harmonics at the output yield a perception of the original low pitch. As was mentioned previously, unless the input to this NLD is a single frequency, intermodulation distortion will occur. In most practical situations this is not really a problem, which is probably partly due to the masking effect of the rest of the audio signal. However, in some situations, artefacts can occur which might be due to this intermodulation distortion. Therefore, when choosing a specific NLD, one of the criteria is to explore its behaviour in this respect. In Secs. 4.2 and 4.3 some specific examples are presented.

4.1.3 Second bandpass filter (BP2)

The input to this filter is the harmonics signal, where the specific spectrum of this signal will of course depend on the choice of the harmonics generator. This filter is used to shape the spectrum to yield a natural sounding timbre of the enhanced bass, and the filter transfer function should be tuned depending on the loudspeaker as well as the NLD.

4.2 Full wave rectifier

Following the block scheme of Fig. 1, a possibility would be a full wave rectification of the input signal. The advantage here is the simplicity in processing. For a sine wave input only even harmonics are generated (in App. A expressions for the complete output signal given an arbitrary periodic input signal are given). So for an input of frequency f_0 , we get $2f_0$, $4f_0$, $6f_0$, etc., at the output; this is a signal with a fundamental of $2f_0$ and thus the pitch will not correspond to the original f_0 . Actually, this is the heterodyning mentioned in Sec. 3.1 and can give good results for some, but not all, repertoire. Fig. 5 shows an input signal (solid line), which leads to an output signal given by the dashed line for the full wave rectifier. Fig. 6 shows the frequency components: an input of f_0 gives output frequencies $2f_0$, $4f_0$, etc., with a relatively rapid decay.

4.3 Full wave integrator

To create a deeper bass impression, corresponding to the pitch of the original fundamental, we must create a harmonics signal containing all (odd and even) harmonics.

This is possible by using a ‘full wave integrator’. This non-linear device integrates the absolute value of the input, and the output is reset to zero when the input has a zero crossing with a positive slope. For a sine wave input the situation is shown in Fig. 5, the full wave integrator output is shown as the dash-dotted signal. Fig. 6 shows the input and output spectra: the output contains all harmonics which decay relatively slowly. As was tested on a real-time prototype system running on a workstation, the full wave integrator indeed yields a much deeper bass impression than the full wave rectifier.

To explore what happens when the input signal is not a single frequency, but a more realistic (musical) signal, consider the following: the locations of the zero crossings are very important (as the output signal is reset to zero at every zero crossing with positive slope) and determine the fundamental frequency of the output signal, which should ideally be the same as the fundamental frequency of the input signal. If we consider a weakly stationary time series with spectral distribution $F(\omega)$, we can then write, as is shown in Kedem [21],

$$\cos \pi \gamma = \frac{\int_0^\pi \cos \omega \, dF(\omega)}{\int_0^\pi dF(\omega)}, \quad (14)$$

where γ is the expected zero crossing rate of the signal, i.e. the expected number of zero crossings in a certain interval (which is e.g. 2 per period for a sine). This is called the *zero crossing spectral representation* and it expresses the tendency of $\pi \gamma$ to be attracted to a specific frequency (band), if this frequency (band) is dominant in the signal. This is a well known empirical fact known as the *dominant frequency principle*. It shows us that we can be confident that if an input signal has a dominant frequency component, this will be reflected in its zero crossings. Consequently this frequency component will be the fundamental frequency of the output of the full wave integrator. Exact expressions for the output as function of an arbitrary periodic input signal (and also for discrete-time signals) are given in App. A.

5 Conclusions

The proposed signal processing scheme shown in Fig. 1 leads to a significant enhancement of perceived bass, without radiating energy in this bass frequency region. This is achieved by exploiting psychoacoustic phenomena. The method can be tuned to any loudspeaker which does not reproduce the lowest audible frequencies. The main advantages are that a greater bass enhancement is possible than with traditional equalization or boosting. In addition this method is much more power efficient, which makes it especially attractive for portable applications. The system is not meant to replace good quality, large loudspeakers, but in many situations it is not possible to use these, and then the proposed type of processing can certainly increase the performance of the loudspeaker.

6 Acknowledgements

The authors would like to thank present respectively former colleagues Catherine Polisset and Erik van der Tol for their parts in the work presented in this paper. We would also like to acknowledge dr. A. Janssen for providing great help in the mathematical derivations presented in App. A and, together with the colleagues of the Acoustics & Sound Reproduction cluster, for their useful comments on the manuscript.

A Analysis of harmonics generation

A.1 Introduction

In this section, we derive analytical descriptions for the full wave rectifier and the full wave integrator. Obviously this requires a different approach than the one used for linear time-invariant (LTI) systems, and in general, descriptions of non-linear systems are extremely complex or pertain to a limited class of signals. However, for our purposes, an elegant description has been obtained that encompasses all practical signals.

Firstly, consider a real periodic signal $f(t)$, having a period of 1, and assume that

- $$\begin{aligned} f(0) = f(t_0) = f(1) = 0, \\ f(t) \neq 0, t \neq 0, t_0, 1, \end{aligned} \quad (15)$$

Thus $f(t)$ has one zero, at t_0 , in the interval $(0, 1)$.

- $f(t)$ changes sign at every zero crossing.
- We choose $f'(0) > 0$.
- $f(t)$ is sufficiently smooth in order that its Fourier coefficients a_n (Eqn. 16) decay at a rate of at least $1/n^2$ (which will be satisfied if $f(t)$ is twice continuously differentiable).

We have for $f(t)$ the Fourier series representation

$$f(t) = \sum_{n=-\infty}^{\infty} a_n e^{2\pi i n t}, \quad (16)$$

where $a_n = a_{-n}^*$, because $f(t)$ is real (x^* represent the complex conjugate of x). Now we also consider the real periodic function $F(t)$, derived from $f(t)$ by some non-linear operation. We have for $F(t)$ the Fourier series representation

$$F(t) = \sum_{n=-\infty}^{\infty} b_n e^{2\pi i n t}, \quad (17)$$

where $b_n = b_{-n}^*$. In the following, we derive expressions for the b_n in terms of the a_n , where each subsection covers a different non-linear operator (and hence the b_n in the various subsections are not the same). More specifically, it is shown that the b_n obtained by full wave rectification of $f(t)$ decay as $1/n^2$ and, for large n , can be expressed in the values of $f'(t)$ at the zero crossings of $f(t)$. For the full wave integrator, the b_n decay as $1/n$ and are mainly determined by the area between $f(t)$ and the horizontal axis.

A.2 Full wave rectifier

The first non-linear device that we treat is the full wave rectifier (see Sec. 4.2). On the periodicity interval $[0, 1)$ the function $F(t)$ is now given by

$$F(t) = |f(t)| \quad , \quad 0 \leq t < 1. \quad (18)$$

Now there holds

$$|f(t)| = f(t)h(t; 0, t_0, 1) \quad , \quad 0 \leq t < 1, \quad (19)$$

where

$$h(t; 0, t_0, 1) = \begin{cases} 1 & , \quad 0 \leq t < t_0, \\ -1 & , \quad t_0 < t < 1. \end{cases} \quad (20)$$

Letting d_n be the Fourier coefficients of $h(t; 0, t_0, 1)$, so that

$$h(t; 0, t_0, 1) = \sum_{n=-\infty}^{\infty} d_n e^{2\pi i n t}, \quad (21)$$

we then obtain from Eqns. 16, 19 and 21 that

$$F(t) = \sum_{n=-\infty}^{\infty} a_n e^{2\pi i n t} \cdot \sum_{m=-\infty}^{\infty} d_m e^{2\pi i m t} = \sum_{k=-\infty}^{\infty} e^{2\pi i k t} \cdot \sum_{n+m=k} a_n d_m, \quad (22)$$

hence from Eqn. 17

$$b_k = \sum_{n=-\infty}^{\infty} a_n d_{k-n}. \quad (23)$$

Due to the piecewise constant nature of $h(t)$ it is easily computed that

$$d_0 = \int_0^1 h(t; 0, t_0, 1) dt = 2t_0 - 1, \quad (24)$$

$$\begin{aligned} d_n &= \int_0^1 h(t; 0, t_0, 1) e^{-2\pi i n t} dt \\ &= \frac{1}{\pi i n} (1 - e^{-2\pi i n t_0}), \quad n \neq 0. \end{aligned} \quad (25)$$

Therefore, from Eqns. 23, 24 and 25

$$b_k = (2t_0 - 1)a_k + \sum_{n \neq k} \frac{a_n}{\pi i(k-n)} (1 - e^{2\pi i(n-k)t_0}). \quad (26)$$

In principle this solves the problem for the full wave rectifier: we have expressed the b_k in terms of the a_k and the locations of the zeros of $f(t)$. However, the right-hand side of Eqn. 26 shows a decay of the b_k roughly as $1/k$, while we know from the form of $F(t)$ that there should be a decay like $1/k^2$ due to the triangular singularity of $F(t)$ at $t = t_0$. This decay of the b_k can be obtained when we properly use the condition stated in Eqn. 15. Accordingly, we have

$$\sum_{n=-\infty}^{\infty} a_n = 0, \quad \sum_{n=-\infty}^{\infty} a_n e^{2\pi i n t_0} = 0. \quad (27)$$

Then we get for the series at the far right-hand side of Eqn. 26

$$\begin{aligned} \sum_{n \neq k} \frac{a_n}{\pi i(k-n)} (1 - e^{2\pi i(n-k)t_0}) &= \sum_{n \neq k} \frac{a_n}{\pi i} \left(\frac{1}{k-n} - \frac{1}{k} + \frac{1}{k} \right) (1 - e^{2\pi i(n-k)t_0}) \\ &= \sum_{n \neq k} \frac{n a_n}{\pi i k(k-n)} (1 - e^{2\pi i(n-k)t_0}) + \\ &\quad \frac{1}{\pi i k} \sum_{n \neq k} a_n (1 - e^{2\pi i(n-k)t_0}), \quad k \neq 0. \end{aligned} \quad (28)$$

Now it holds that

$$\begin{aligned} \sum_{n \neq k} a_n e^{2\pi i(n-k)t_0} &= -a_k + \sum_{n=-\infty}^{\infty} a_n e^{2\pi i(n-k)t_0} \\ &= -a_k + e^{-2\pi i k t_0} \sum_{n=-\infty}^{\infty} a_n e^{2\pi i n t_0} \\ &= -a_k. \end{aligned} \quad (29)$$

and in the same way we have that $\sum_{n \neq k} a_n = -a_k$. Hence, for $k \neq 0$, the second term of Eqn. 28 vanishes, and we find

$$b_0 = \int_0^1 |f(t)| dt, \quad (30)$$

$$b_k = (2t_0 - 1)a_k - \sum_{n \neq k} \frac{n a_n}{\pi i k(k-n)} (1 - e^{2\pi i(n-k)t_0}). \quad (31)$$

The right-hand side of Eqn. 31 does exhibit the correct $1/k^2$ behaviour that we expect from the b_k 's for large k (since the a_k also decay at a rate of at least $1/k^2$

as explained in the introduction to this appendix). More precisely, assuming that $a_k = 0$ for large k , we have for large k that

$$\sum_{n \neq k} \frac{na_n}{\pi i k(k-n)} (1 - e^{2\pi i(n-k)t_0}) \approx \frac{1}{k^2} \sum_{n=-\infty}^{\infty} \frac{na_n}{\pi i} (1 - e^{2\pi i(n-k)t_0}). \quad (32)$$

Since

$$f'(t) = \sum_{n=-\infty}^{\infty} 2\pi i n a_n e^{2\pi i n t}, \quad (33)$$

we then obtain

$$\begin{aligned} \sum_{n \neq k} \frac{na_n}{\pi i k(k-n)} (1 - e^{2\pi i(n-k)t_0}) &\approx \frac{1}{k^2} \frac{1}{\pi i} \frac{1}{2\pi i} \sum_{n=-\infty}^{\infty} 2\pi i n a_n (1 - e^{2\pi i(n-k)t_0}) \\ &= -\frac{1}{2\pi^2 k^2} (f'(0) - f'(t_0) e^{-2\pi i k t_0}). \end{aligned} \quad (34)$$

Thus, if $a_k = 0$ for large k , then for large k

$$b_k \sim \frac{1}{2\pi^2 k^2} (f'(0) - f'(t_0) e^{-2\pi i k t_0}). \quad (35)$$

A.3 Full wave integrator

Now we consider the full wave integrator (see Sec. 4.3), on the periodicity interval $[0, 1)$. We get

$$F(t) = \int_0^t |f(s)| ds, \quad 0 \leq t < 1, \quad (36)$$

The jumps of $F(t)$ at the resetting moments are given by

$$-\alpha_0 = -\int_0^1 |f(s)| ds \quad \text{at time } t = k, \quad k \in \mathbb{Z}. \quad (37)$$

For $t \neq 0, t_0, 1$, we have that $F'(t) = |f(t)|$, thus

$$F'(t) = |f(t)| - \alpha_0 \sum_{n=-\infty}^{\infty} \delta(t - n). \quad (38)$$

Denoting the Fourier coefficients of $|f(t)|$ by c_k , so that

$$|f(t)| = \sum_{k=-\infty}^{\infty} c_k e^{2\pi i k t}, \quad (39)$$

and using $\sum_{n=-\infty}^{\infty} \delta(t - n) = \sum_{k=-\infty}^{\infty} e^{2\pi i k t}$ we can write Eqn. 38 as

$$\sum_{k=-\infty}^{\infty} 2\pi i k b_k e^{2\pi i k t} = \sum_{k=-\infty}^{\infty} (c_k - \alpha_0) e^{2\pi i k t}, \quad (40)$$

so that

$$b_k = \frac{c_k - \alpha_0}{2\pi i k}, \quad k \neq 0. \quad (41)$$

The b_k show a decay of roughly $1/k$, which is what we expect due to the discontinuity of $F(t)$ at $t = 1$. The c_k can be found using the expressions of the previous subsection. For $k = 0$, and using partial integration, we obtain

$$\begin{aligned} b_0 &= \int_0^1 F(t) dt \\ &= [tF(t)]_0^1 - \int_0^1 t \left(|f(t)| - \alpha_0 \sum_{n=-\infty}^{\infty} \delta(t-n) \right) dt \\ &= \int_0^1 (1-t)|f(t)| dt. \end{aligned} \quad (42)$$

A.4 Generalization to arbitrary periodic signals

We can generalize the above results for arbitrary periodic signals that may have more than one zero crossing in the fundamental period. The derivations follow exactly the same procedure as given above, with the following considerations:

- The start and end point of a period are now t_{-1} and t_z respectively; in between there are z zeros at $t_{0,1\dots z-1}$. Due to the periodicity requirements and the fact that $f(t)$ changes sign at every zero, z must be odd.
- The fundamental frequency of the signal is $\nu_0 = 1/(t_z - t_{-1})$.
- For the full wave integrator $F(t)$ is reset to zero at $t_{1,3\dots z}$, the corresponding jumps are given by $\alpha_{0,1\dots(z-1)/2}$.

An example signal with the t_m indicated is shown in Fig. 7, for the case $z = 7$. The result for the full wave rectifier follows as

$$b_0 = \nu_0 \int_{t_{-1}}^{t_z} |f(t)| dt, \quad (43)$$

$$b_k = (1 + 2\nu_0 \sum_{m=0}^z (-1)^m t_m) a_k - \sum_{n \neq k} \frac{n a_n}{\pi i k (k-n)} \sum_{m=0}^z (-1)^m e^{2\pi i \nu_0 (n-k) t_m}, \quad (44)$$

and if $a_k = 0$ for large k , we then get for large k

$$b_k \sim \frac{1}{2\pi^2 \nu_0 k^2} \sum_{m=0}^z (-1)^m f'(t_m) e^{-2\pi i \nu_0 k t_m}. \quad (45)$$

For the full wave integrator (and denoting the Fourier coefficients of the full wave rectified signal by c_k), we get

$$b_k = \frac{c_k - \sum_{m=0}^{(z-1)/2} \alpha_m e^{-2\pi i \nu_0 k t_{2m+1}}}{2\pi i \nu_0 k}, \quad k \neq 0. \quad (46)$$

$$b_0 = - \int_{t_{-1}}^{t_z} t |f(t)| dt + \sum_{m=0}^{(z-1)/2} \alpha_m t_{2m+1}. \quad (47)$$

A.5 Discrete time

We can derive expressions for sampled signals as well (amplitude-continuous). We use square brackets to indicate the time-discrete property of the signals, e.g. $f[n]$. The number of samples per period is N , the sample time Δt , and the n_m ($m = -1, 0 \dots z$) are the zero crossings of $f[n]$, analogously as in the continuous time case. We define a zero crossing in the discrete-time sequence to occur at n_m if $f[n]$ changes sign at $n = n_m$ (or if $f[n_m] = 0$).

For the full wave rectified signal we get

$$b[k] = \left(1 + \frac{2}{N} \sum_{m=0}^z (-1)^m n_m\right) a[k] + \frac{1}{N} \sum_{n \neq k} a[n] \sum_{m=0}^z (-1)^m e^{-\pi i (n_{m-1} + n_m - 1)(k-n)/N} \frac{\sin \pi (n_m - n_{m-1})(k-n)/N}{\sin \pi (k-n)/N}. \quad (48)$$

For the full wave integrator (using $c[k]$ for the full wave rectified signal) the $b[k]$ become

$$b[k] = \Delta t \frac{c[k] - \sum_{m=0}^{(z-1)/2} \alpha_m e^{-2\pi i k n_{2m+1}/N}}{1 - e^{-2\pi i k/N}}, \quad k \neq 0. \quad (49)$$

$$b[0] = -\Delta t \sum_{k=n_{-1}}^{n_z-1} k |f[k]| + \Delta t \sum_{m=0}^{(z-1)/2} \alpha_m n_{2m+1}. \quad (50)$$

In the limit that $\Delta t \downarrow 0$, the discrete time and continuous time expressions are expected to become identical. By substituting $N = 1/(\Delta t \nu_0)$ and $\Delta t n_m = t_m$ in Eqns. 48, 49 and 50 and taking the limit $\Delta t \downarrow 0$ it can be seen that this is indeed the case.

References

- [1] R.M. Aarts. *25 jaar AES in Nederland*, chapter 17, pages 158–159. Gebotekst, Zoetermeer, The Netherlands, 1999.
- [2] H.F. Olson. *Acoustical Engineering*. Van Nostrand, Princeton, New Jersey, 1957.
- [3] L.L. Beranek. *Acoustics*. American Institute of Physics, New York, 1954. 1986 reprint for the Acoust. Soc. Am.
- [4] J. Borwick, editor. *Loudspeaker and headphone handbook*. Butterworths, London, 1988.
- [5] T. Unemura. Audio circuit, 1998. US patent 5,771,296.
- [6] M. Oda. Low frequency audio conversion circuit, 1997. US patent 5,668,885.
- [7] W. Schott. Low frequency audio doubling and mixing circuit, 1991. European patent EP0546619.
- [8] R.M. Aarts. Circuit, audio system and method for processing signals, and a harmonics generator, 1996. European patent EP0843951. Priority date May 8th 1996.
- [9] H. Helmholtz. *Die Lehre von den Tonempfindungen*. Friedr. Vieweg & Sohn, Dover, 1913. The first printing: 1863, English translation of the 4th German edition of 1877.
- [10] J.G. Roederer. *Introduction to physics and psychophysics of music*. Springer, New York, 1975.
- [11] E. Terhardt and M. Seewan. Der ‘akustische Bass’ von Orgeln. In *Fortschritte der Akustik DAGA84*, pages 885–888, Darmstadt, 1999. DeGA.
- [12] R. Plomp. *Experiments on tone perception*. PhD thesis, University of Utrecht, 1966.
- [13] F.A. Bilsen and R.J. Ritsma. Some parameters influencing the perceptibility of pitch. *J. Acoust. Soc. Am.*, 47(2 (Part 2)):469–475, 1970.
- [14] E. de Boer. *On the ‘residue’ in hearing*. PhD thesis, University of Amsterdam, 1956.
- [15] A.J.M. Houtsma and J.L. Goldstein. The central origin of the pitch of complex tones: Evidence from musical interval recognition. *J. Acoust. Soc. Am.*, 51(2 (Part 2)):520–529, 1972.

- [16] R.J. Ritsma. Existence region of the tonal residue I. *J. Acoust. Soc. Am.*, 34(9):1224–1229, 1962.
- [17] R.J. Ritsma. Existence region of the tonal residue II. *J. Acoust. Soc. Am.*, 35(8):1241–1245, 1963.
- [18] J.F. Schouten. The perception of pitch. *Philips Technical Review*, 5(10):286, 1940.
- [19] J.F. Schouten, R.J. Ritsma, and B. Lopes Cardozo. Pitch of the residue. *J. Acoust. Soc. Am.*, 34(8 (Part 2)):1418–1424, 1962.
- [20] D. Ben-Tzur and M. Colloms. The effect of MaxxBass psychoacoustic bass enhancement on loudspeaker design. In *preprint 4892(F3) of the 106th AES Convention Munich*. Audio Eng. Soc., May 1999.
- [21] B. Kedem. *Time series analysis by higher order crossings*. IEEE Press, New York, 1994.
- [22] International standard ISO 226-1987(E), 1987. Acoustics – normal equal-loudness level contours.

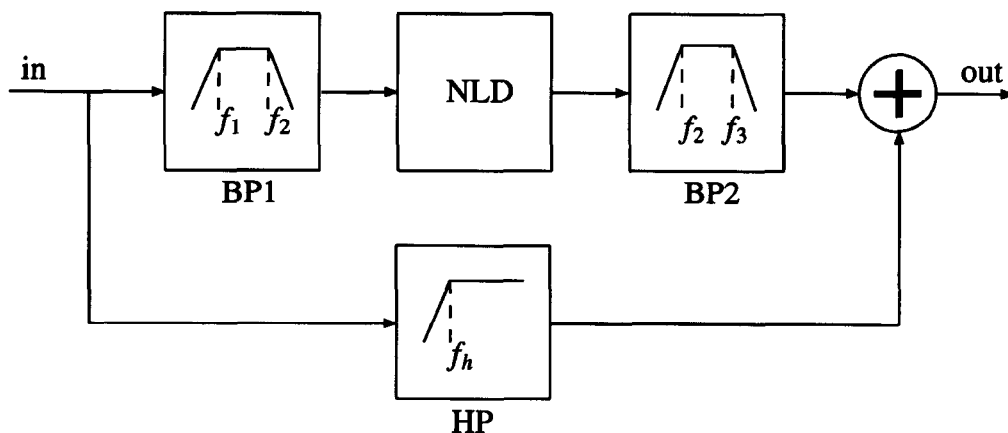


Figure 1: *Block scheme for psychoacoustic bass enhancement. In the upper branch, frequencies which are too low to be reproduced by the loudspeaker are transposed to a higher frequency region. In the lower branch, the input is optionally highpass filtered. The output signal will now be perceived to have a higher bass content.*

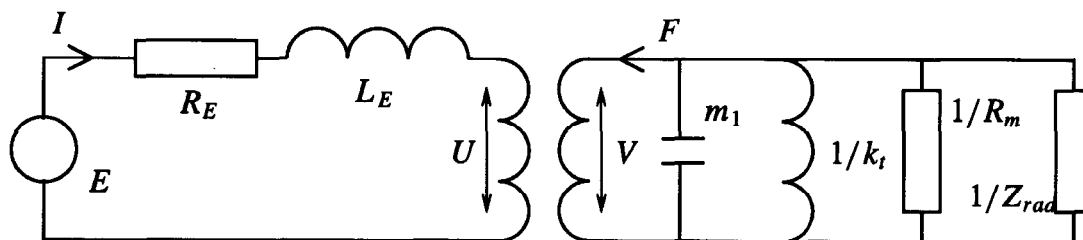


Figure 2: *The mobility analogous circuit for an electrodynamic loudspeaker in a box driven by generator E . The electrodynamic coupling follows $U = BlV$ and $F = BlI$. The symbols are explained in the text.*

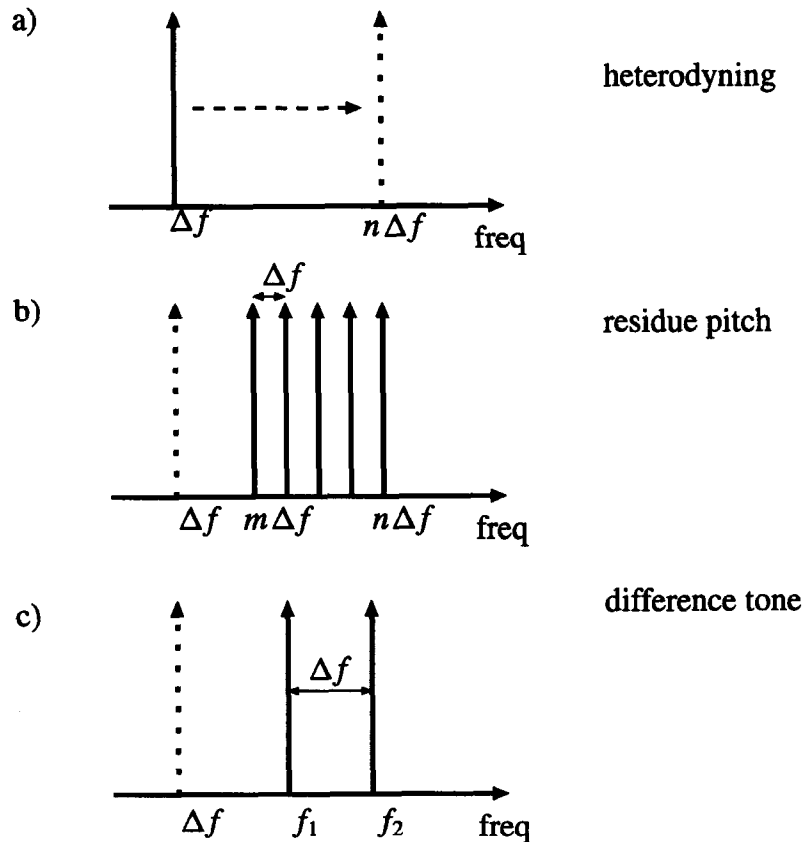


Figure 3: *Possible options for psychoacoustic bass enhancement. The dotted frequency component denotes the perceived pitch (but is not necessarily acoustically radiated).*

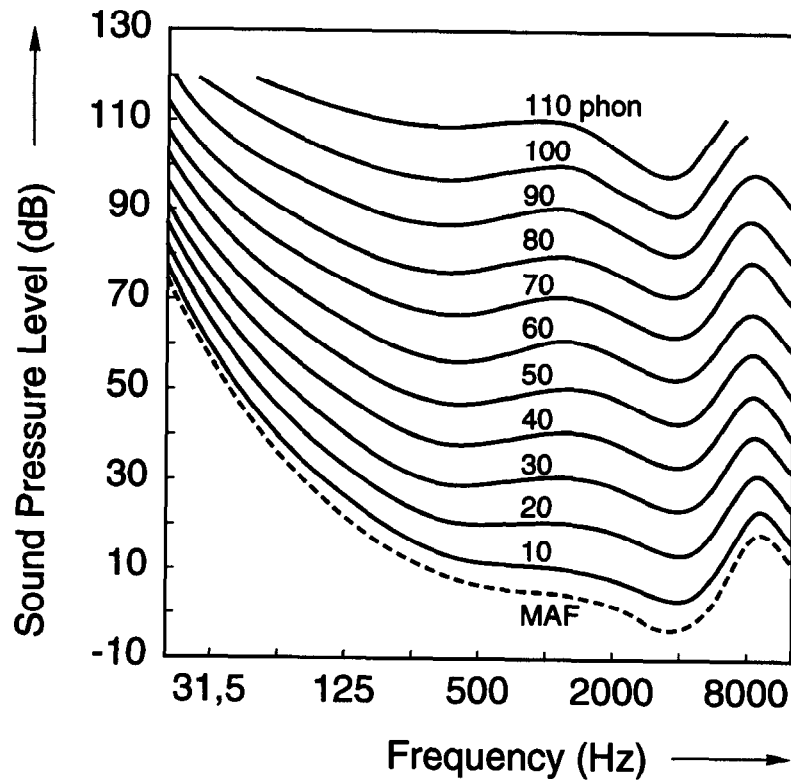


Figure 4: *Equal-loudness level contours for pure tones (binaural free-field listening, frontal incidence), from [22] Fig. 1.*

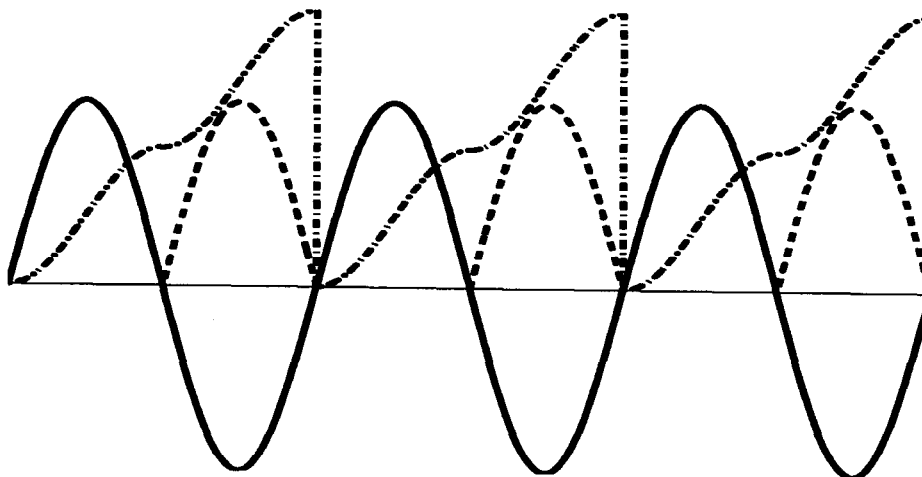


Figure 5: *The solid line represents a sine wave input. The dashed line is obtained by full wave rectification, the dash-dotted line by full wave integration.*

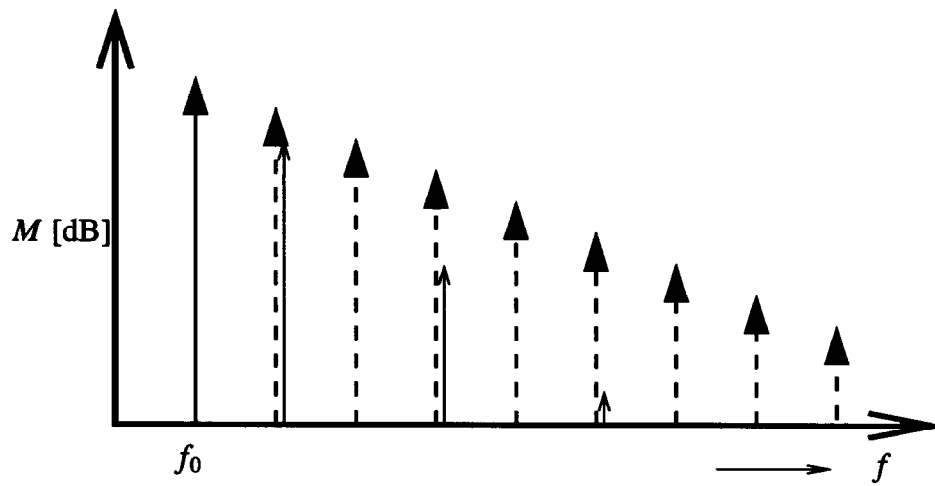


Figure 6: *The solid arrow at f_0 represents the input spectrum. The arrows at $2f_0, 4f_0, \text{etc.}$, represent the output spectrum for the full wave rectifier, the dashed arrows at $2f_0, 3f_0, \text{etc.}$, represent the output spectrum for the full wave integrator.*

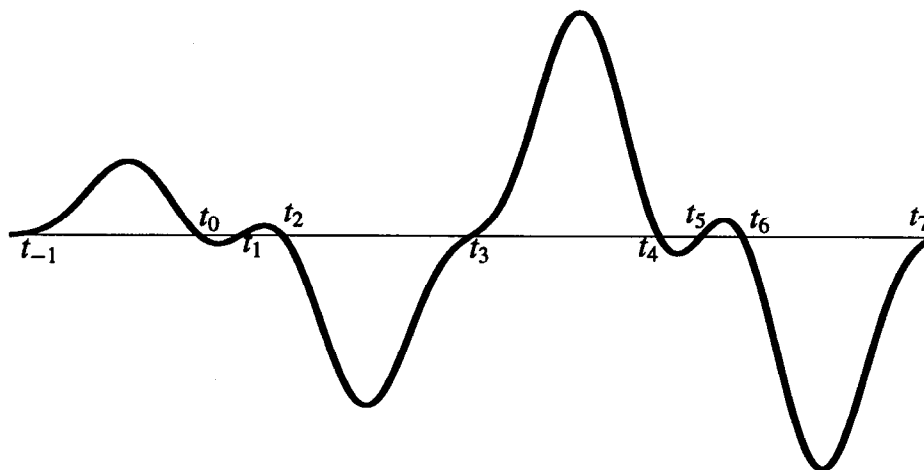


Figure 7: *An arbitrary periodic signal with the zeros indicated in the notation of App. A. In this case $z = 7$.*